

Supplementary Information

Simple and Cost Effective Fabrication of 3D Porous Core-shell Ni Nanochains@NiFe Layered Double Hydroxide Nanosheets Bifunctional Electrocatalysts for Overall Water Splitting

Zhengyang Cai,^{a,1} XiuMing Bu,^{b,1} Ping Wang,^{a,c,*} Wenqiang Su,^a Renjie Wei,^b Johnny C. Ho,^{b,*} Junhe Yang,^{a,c} Xianying Wang^{a,c,*}

^a School of Materials Science and Technology, University of Shanghai for Science and Technology, Jungong Rd.516, 200093 Shanghai, P.R. China. Email: ping.wang@usst.edu.cn; xianyingwang@usst.edu.cn

^b Department of Materials Science and engineering, City University of Hong Kong, 83 Tat Chee Avenue, Kowloon, Hong Kong, P.R. China. Email: johnnyho@cityu.edu.hk

^c Shanghai Innovation Institute for Materials, 200444 Shanghai, P.R. China.

¹ These authors contributed equally to the work.

Experimental Section

Chemicals: The chemicals were used as received without further purification. Hydrochloric acid (HCl, AR, Adamas, Shanghai, P.R. China), ethanol (C₂H₆O, ≥ 99.7 %, Adamas, Shanghai, P.R. China), Sodium citrate dehydrate (C₆H₅Na₃O₇·2H₂O, ≥ 99.0 %, Aladdin Co., P.R. China), Nickel chloride hexahydrate (NiCl₂·6H₂O, AR, Aladdin Co., P.R. China), Hydrazine monohydrate (N₂H₄·H₂O, > 98.0 %, Aladdin Co., P.R. China), Nickel(II) nitrate hexahydrate (Ni(NO₃)₂·6H₂O, 98 %, Aladdin Co., P.R. China), Ferrous(II) sulfate heptahydrate (FeSO₄·7H₂O, 99.95 %, Aladdin Co., P.R. China), Nafion D-521 solution (5 %, Alfa Aesar), Ruthenium(IV) oxide (RuO₂, 99.95 %, Adamas, Shanghai, P.R. China), Iridium(IV) Oxide (IrO₂, 99.9 %, Adamas, Shanghai, P.R. China), Platinum on carbon (20 wt. % Pt/C, Sigma-Aldrich, Germany), Potassium hydroxide (KOH, ACS, Aladdin Co., P.R. China), and Ni foam (1.0 mm in thickness, surface area of ~1.9 m²·g⁻¹, Tianjin EVS Co., P.R. China). Deionized (DI) water with a resistance of ~18.2 MΩ was used throughout all experiments.

Fabrication of Ni nanochains (Ni NCs): The *in-situ* growth of Ni NCs on Ni foam was carried out by a modified magnetic field-assisted chemical reduction method. Typically, a piece of Ni foam with the area of $3 \times 3 \text{ cm}^2$ was cleaned in hydrochloric acid (37 wt%) and rinsed with ethanol and DI water for several times sequentially. Specifically, 50 mL of aqueous solution containing $\text{NiCl}_2 \cdot 6\text{H}_2\text{O}$ (0.05 M), $\text{Na}_3\text{C}_6\text{H}_5\text{O}_7 \cdot 2\text{H}_2\text{O}$ (0.02 M) was heated at $75 \text{ }^\circ\text{C}$, followed by adding 2.1 mL of hydrazine monohydrate. Subsequently, the Ni foam was placed vertically to the magnetic field direction. After 90 mins, the obtained Ni NCs sample was washed sequentially by ethanol and DI water each for 5 min. Each of those was then cut into 6 pieces with a working area of $1 \times 1 \text{ cm}^2$ for use.

Fabrication of Ni@NiFe LDH: The NiFe LDH nanosheets were electrically deposited on surface of Ni NCs by in a standard three-electrode system equipped with Ni NCs, Pt plate and Ag/AgCl electrode as the working, counter and reference electrode, respectively. 100 mL of the aqueous solution containing a desired weight ratio of $\text{Ni}(\text{NO}_3)_2 \cdot 6\text{H}_2\text{O}$ and $\text{FeSO}_4 \cdot 7\text{H}_2\text{O}$ precursors was used as electrolyte. The whole system was continuously flowed by high-purity N_2 (5.0 quality) through to avoid the oxidation of Fe^{2+} . In order to promote the deposition of Ni^{2+} and Fe^{2+} , the given potentials resulting from a pulsed electric field was -0.86 V vs. Ag/AgCl for 5 s and -1.1 V vs. Ag/AgCl for the other 5 s. The total cyclic time of 10 s, 50 s or 90 s were investigated to adjust the deposited amount of NiFe LDH. The obtained samples were washed with DI water and dried in air. For comparison, NiFe LDH was deposited on Ni foam by using the same synthetic method for 50 s, denoted as NiFe LDH. The loading amounts of the catalyst in Ni@NiFe LDH for 50 s and NiFe LDH for 50 s are calculated to be about $2.3 \text{ mg} \cdot \text{cm}^{-2}$.

Preparation of RuO_2 , IrO_2 and Pt/C electrodes: The compared electrodes of RuO_2 , IrO_2 and Pt/C were synthesized by using the modified procedures.¹ For example, to prepare the RuO_2 electrode, 40 mg RuO_2 and 60 μL Nafion, 540 μL ethanol and 400 μL DI water were ultrasonicated for homogeneous dispersion. Then, the suspension was coated onto Ni foam, which was then dried at room temperature. The loading amount of RuO_2 , IrO_2 and Pt/C electrode on Ni foam was kept the same amount of $2.3 \text{ mg} \cdot \text{cm}^{-2}$ with those of the Ni@NiFe LDH for 50 s.

Characterizations: The morphology and structure of the as-synthesized samples were detected with scanning electron microscopy (SEM, LEO 1530VP) and transmission electron microscope (TEM, Tecnai G2 F20 S-TWIN) coupled with energy dispersive X-ray spectroscopy (EDS). The phase composition and chemical bonding nature in the samples was characterized by X-ray diffraction (XRD, D8 Advance, Cu K α), Raman spectra (Horiba-Jobin-Yvon T64000 instrument) and Fourier Transform infrared spectroscopy (FTIR, Thermo Nicolet NEXUS 470). Surface chemical compositions of the samples were characterized by an X-ray photoelectron spectroscopy (XPS, AXIS ultra DLD, Shimadzu) in a vacuum of 10^{-7} Pa with an Al K α monochrome anode. The surface area and pore structure of the samples were examined by the Brunauer-Emmett-Teller (BET) model measuring the argon adsorption-desorption isotherms at a liquid nitrogen temperature (Micromeritics, TriStar II 3flex). The samples were degassed at 100 °C for 12 h under a vacuum before the adsorption measurements.

Electrochemical measurements: Electrochemical measurements were carried out on an electrochemical station (Ivium Technologies, Vertex.1A, The Netherlands) in a standard three-electrode system equipped with the as-prepared samples as the working electrode, a 1 cm² carbon paper as the counter electrode, and a standard Hg/HgO electrode as the reference electrode. The OER and HER activities were evaluated using linear sweep voltammetry (LSV) and cyclic voltammetry (CV) methods in 1 M KOH aqueous solution. The overall water splitting performance were evaluated in 1 M KOH aqueous solution using a two-electrode configuration. In order to determine the double-layer capacitance values (C_{dl}), the CV measurements were carried out at different scan rates (from 10 to 100 mV·s⁻¹) in a potential range from 0.98 V to 1.08 V vs. RHE. The stability tests for OER and overall water splitting were performed by chronopotentiometry method at a constant current density of 10 mA·cm⁻² in 1 M KOH aqueous solution for 24 h. Electrochemical impedance spectra (EIS) were measured at an overpotential of 1.48 V vs. RHE from 0.1 Hz to 100 kHz with an amplitude of 10 mV. Notably, all the measured potentials vs. Hg/HgO were converted to RHE by the Nernst equation ($E_{RHE} = E_{Hg/HgO} + 0.0592 \text{ pH} + 0.098$) and except where otherwise stated, an iR compensation of 90 % was applied to all the LSV curves.

Gases evolution measurements: The measurements of H₂ and O₂ evolution were performed in an air-

tight H shape cell. The two as-prepared electrodes were inserted in the chambers of the cell. The cell was filled with 1 M KOH and degassed with high-purity Ar (5.0 quality) for 24 h. The electrolysis was carried out with a constant current density of $200 \text{ mA}\cdot\text{cm}^{-2}$ in 1 M KOH. A measure of 50 mL of the gas sample in the compartment was transferred by a specific syringe to the gas chromatography (GC7900, Techcomp Ltd., Beijing, China, MS-5A column, and high-purity N_2 (5.0 quality) as carrier gas), where the amounts of evolved H_2 and O_2 were determined.

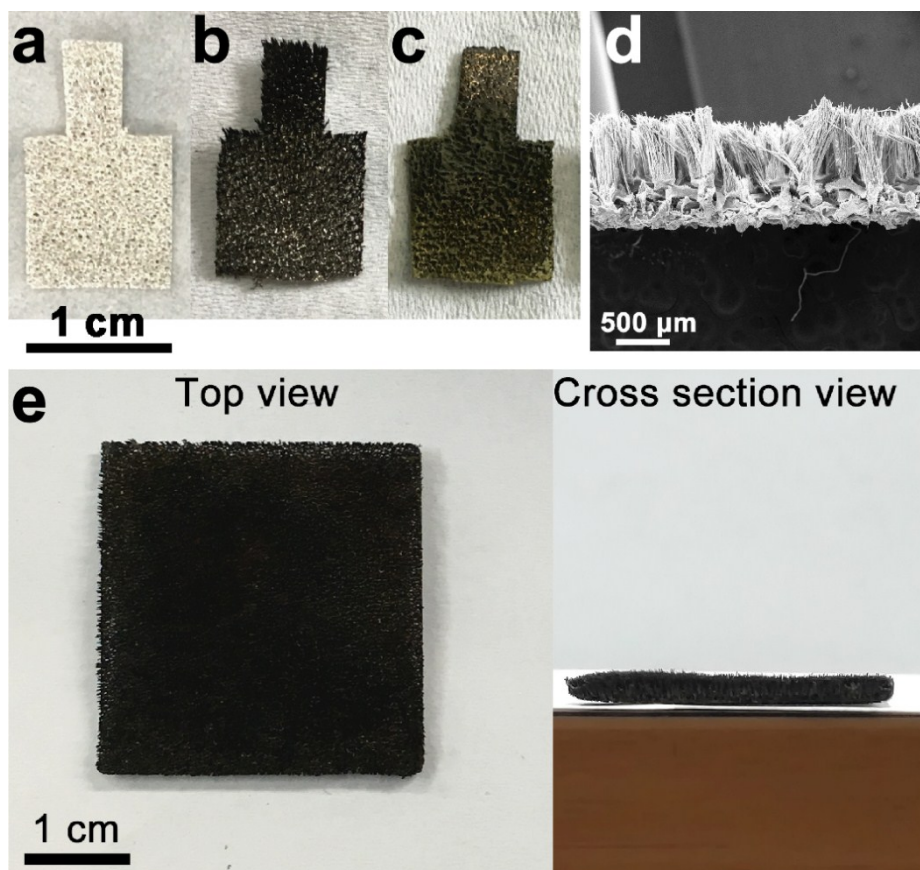


Figure S1. Optical photos of the as-prepared samples: (a) Ni foam, (b) Ni NCs, (c) Ni@NiFe LDH, Cross-section SEM image of Ni@NiFe LDH (d), Top and cross-section optical photos of Ni@NiFe LDH in the size of 3×3 cm (e).

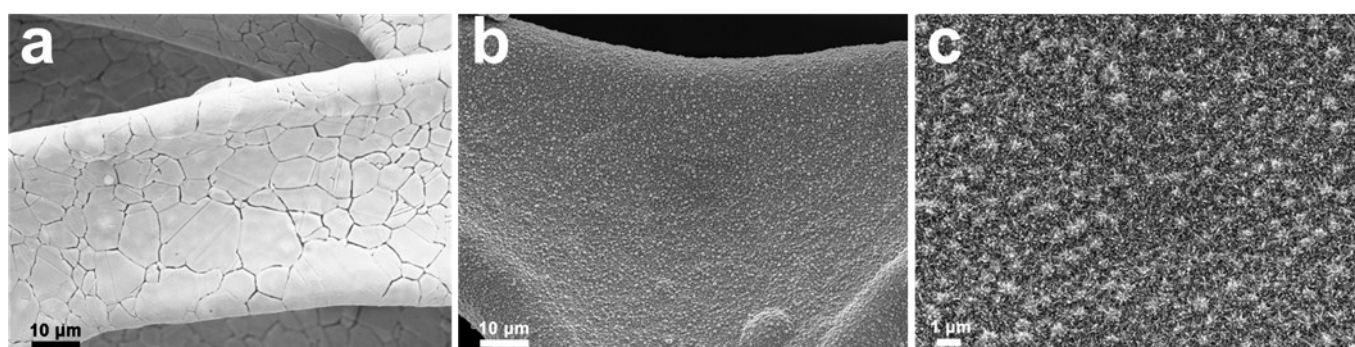


Figure S2. Representative SEM images of pristine Ni foam (a), Ni nanoparticles reduced on Ni foam without application of magnetic fields (b and c).

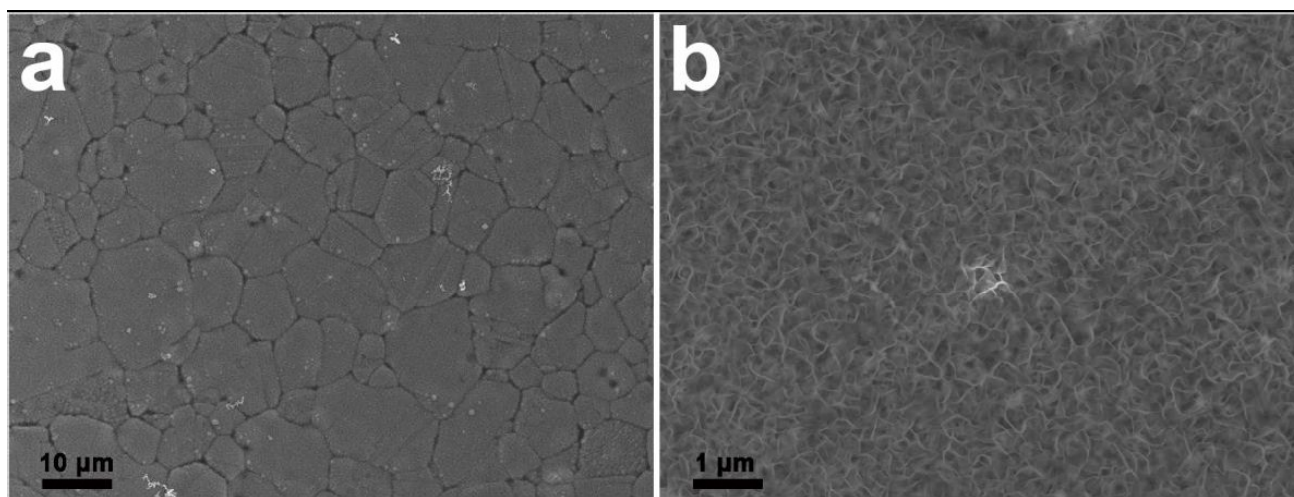


Figure S3. SEM images (a and b) of the as-prepared NiFe LDH sample, in which the NiFe LDH NSs are directly deposited on the Ni foam.

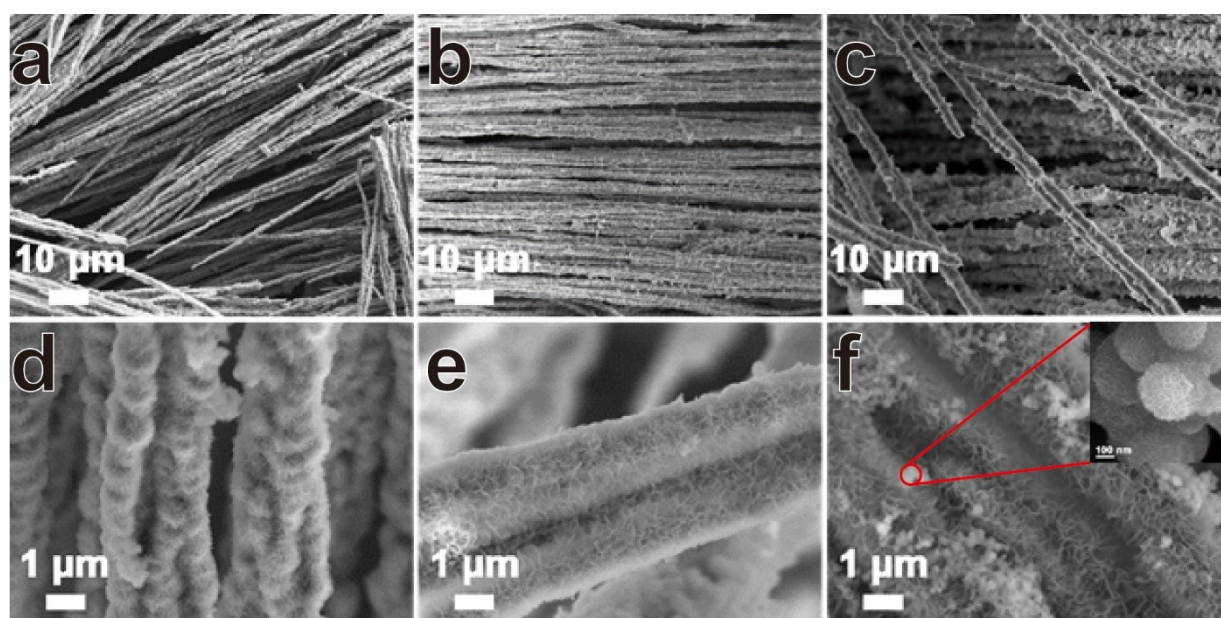


Figure S4. Representative low and high-magnification SEM images of the as-prepared Ni@NiFe LDH samples with different electrodeposition time: (a and d) for 10 s, (b and e) for 50 s and (c and f) for 90 s, the inset in f shows the formation of the nanospheres with the size range of 300 - 360 nm assembled by stacked LDH nanosheets.

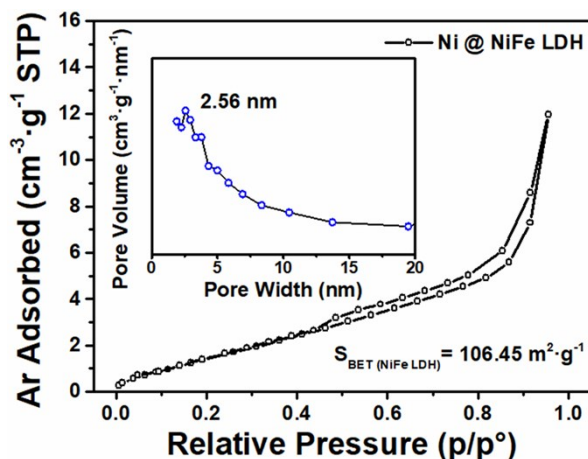


Figure S5. Argon adsorption and desorption isotherms of porous Ni@NiFe LDH, the inset shows the corresponding pore size distribution curve.

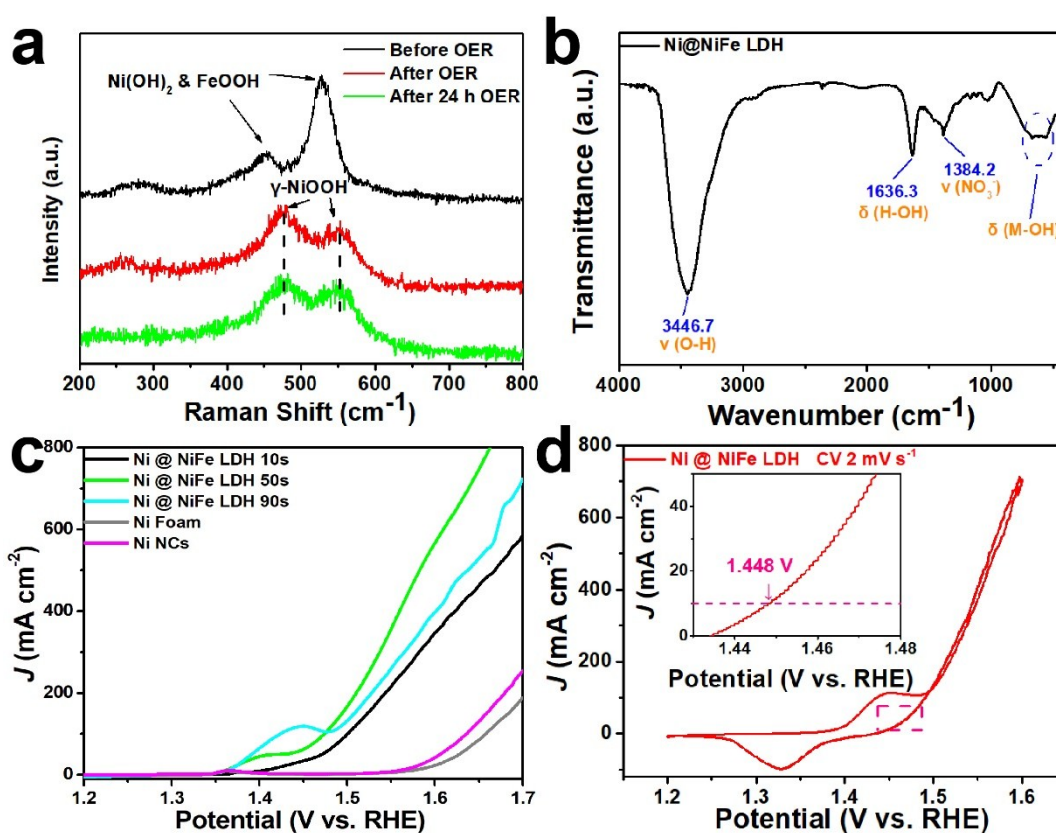


Figure S6. (a) Raman spectra of Ni@NiFe LDH before and after OER operations. (b) FTIR spectrum of the Ni@NiFe LDH. (c) Polarization curves of Ni foam, Ni NCs and Ni@NiFe LDH with different electrodeposition time in 1 M KOH electrolyte for OER, the scan rates are all kept at 5 mV s^{-1} . (d) The CV curve of Ni@NiFe LDH at a scan rate of 2 mV s^{-1} . The inset shows the enlarged view of the dashed box.

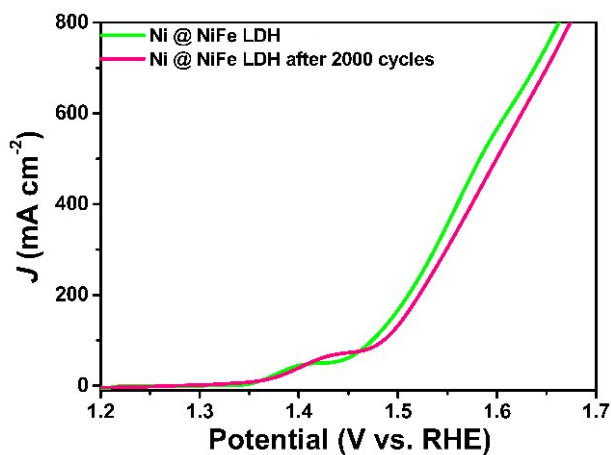


Figure S7. LSV curves for Ni@NiFe LDH before and after 2000 CV cycles, the scan rates are all kept at $5 \text{ mV}\cdot\text{s}^{-1}$.

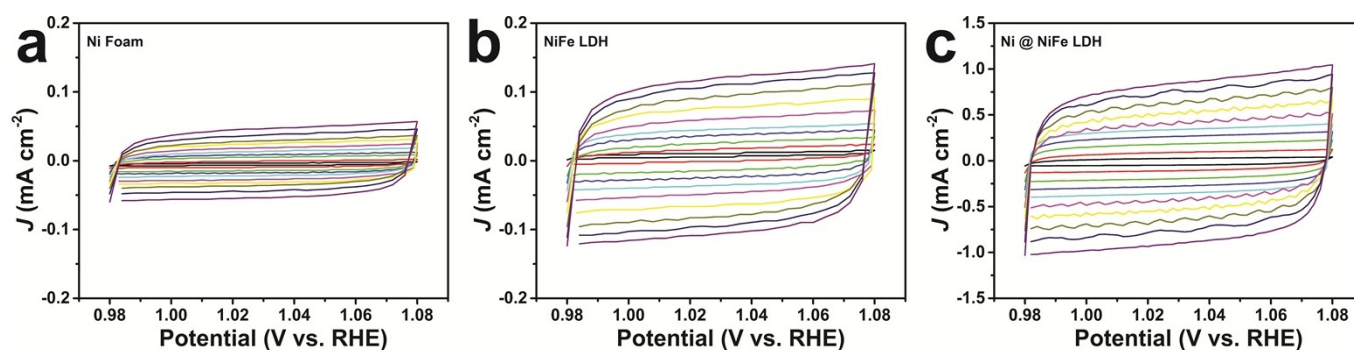


Figure S8. Cyclic voltammograms measured at different scan rates ranging from 10 to $100 \text{ mV}\cdot\text{s}^{-1}$: (a) Ni foam, (b) NiFe LDH, and (c) Ni@NiFe LDH. The scanning potential range is from 0.98 V to 1.08 V vs. RHE with an interval point of $10 \text{ mV}\cdot\text{s}^{-1}$.

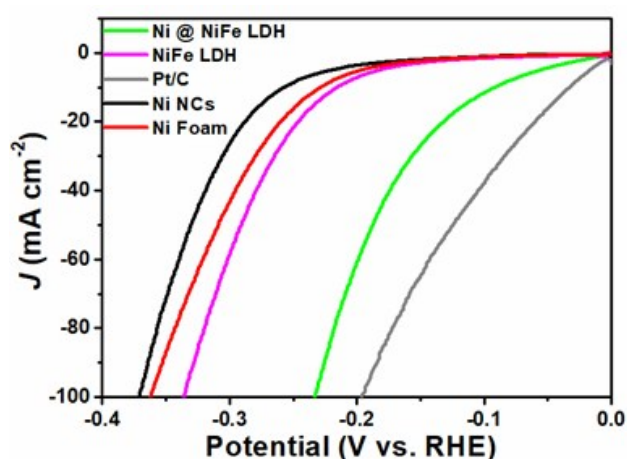


Figure S9. Polarization curves for HER performance of Ni@NiFe LDH, NiFe LDH, Pt/C, Ni NCs and Ni foam, the scan rates are all kept at $5 \text{ mV}\cdot\text{s}^{-1}$.

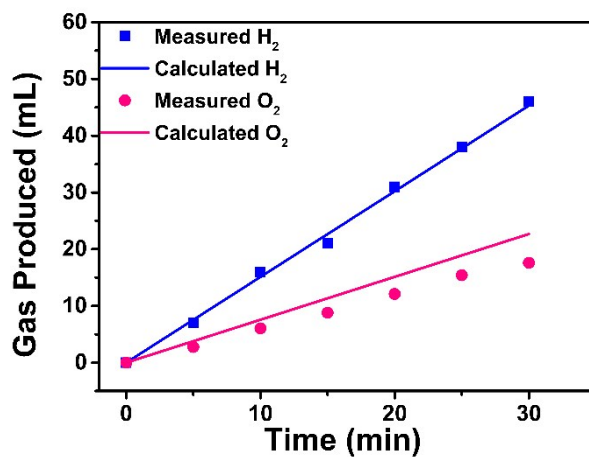


Figure S10. Experimental and theoretical calculated amounts of the evolved H₂ and O₂ over the Ni@NiFe LDH electrodes at a constant current density of 200 mA·cm⁻² in 1 M KOH electrolyte.

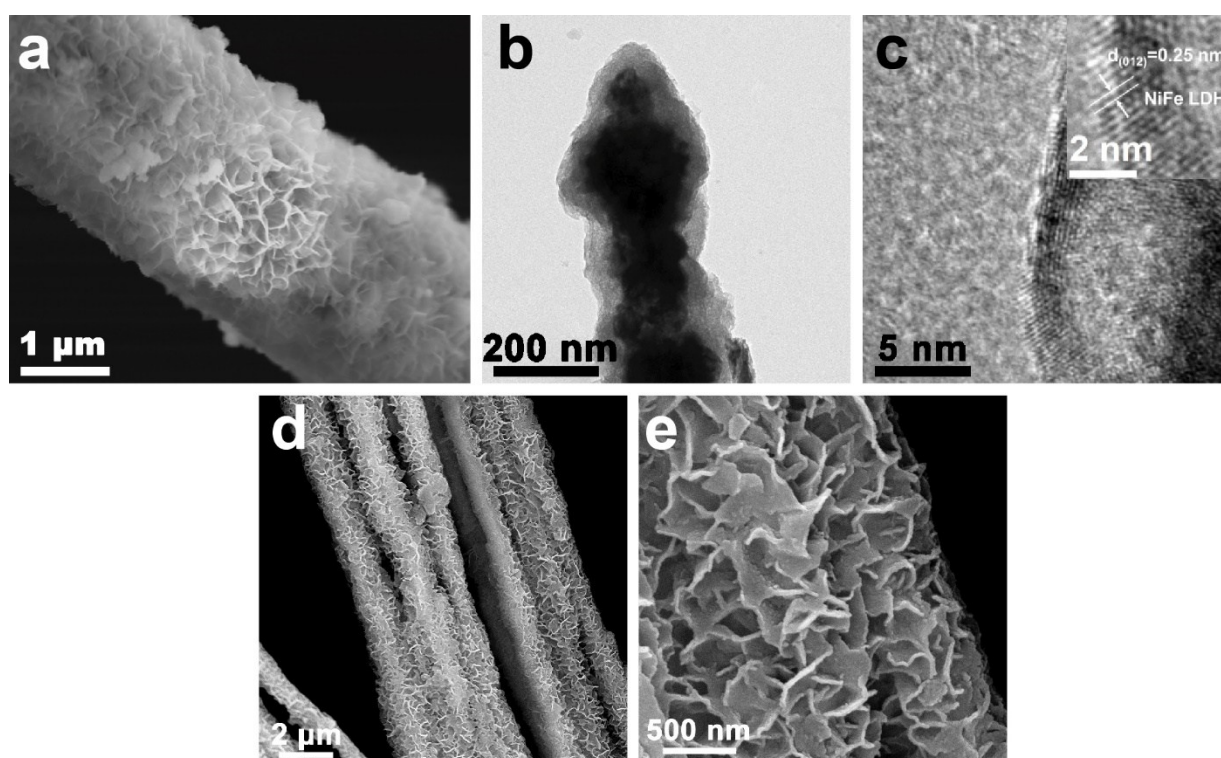


Figure S11. Morphological characterizations of Ni@NiFe LDH after OER stability test for 24h: (a) SEM image, (b) TEM image, and (c) HRTEM image; Low-magnification (d) and high-magnification (e) SEM images of Ni@NiFe LDH after HER stability test for 24h.

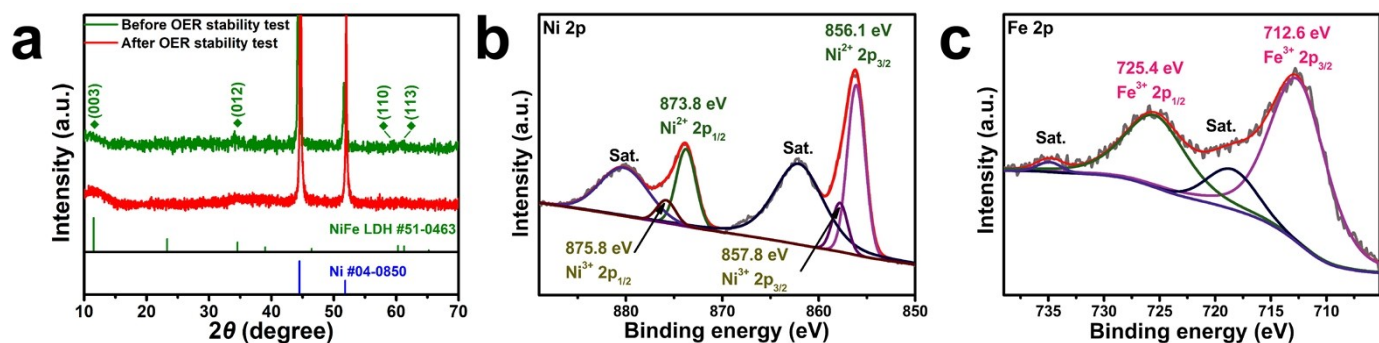


Figure S12. XRD and XPS characterizations of Ni@NiFe LDH before and after the OER stability tests for 24 h. (a) XRD pattern, (b) High-resolution Ni 2p XPS spectra, and (c) High-resolution Fe 2p XPS spectra.

Table S1. Comparison of OER performance for the Ni@NiFe LDH catalyst in the work with other recently reported electrocatalysts in 1 M alkaline electrolytes (KOH or NaOH). η_{10} , η_{100} and η_{300} correspond to the overpotentials at current densities of 10, 100 and 300 $\text{mA} \cdot \text{cm}^{-2}$, respectively.

Catalysts	η_{10} (mV)	η_{100} (mV)	η_{300} (mV)	Tafel Slope ($\text{mV} \cdot \text{dec}^{-1}$)	Substrate	Ref.	Year
Ni@NiFe LDH	218	269	315	66.3	NF¹	The work	
NiFe LDH@NiCoP/NF	220	--	550*	48.6	NF	2	2018
Ni ₅ P ₄ /NiP ₂ /NiFe LDH	197	243	283	46.6	NF	3	2018
NF@Ni/C	265	470	--	54	NF	4	2018
NiCo ₂ P ₂ /GQD NSs	340	400	--	65.9	Ti mesh	5	2018
Cu@CoFe LDH	240	300	--	44.4	Cu Foam	6	2017
NiCo LDH NA/CFP	307	370*	410*	64	CFP ²	7	2016
Ni ₇₆ Co ₂₄ LDHs	293	450*	--	57	NF	8	2016
CoNi LDH/CoO	300	470*	--	123	GC ³	9	2016
NiCo/NiCoO _x @FeOOH	278	430*	--	47.5	NF	10	2017
NiFe LDH HMS	239	320*	--	53	GC	11	2016
NiFe LDH NS@DG10	210	--	--	52	GC	12	2017
Co _{0.85} Se/NiFe LDH/EG	--	260*	290*	57	GF ⁴	13	2016
Ni ₈ Fe LDH@CNTs	220	--	--	34	GC	14	2017
NiFeMn LDH	270	--	--	47	CFP	15	2016
(Ni _{0.5} Fe _{0.5}) ₂ P/Ni foam	203	295*	430*	57	NF	16	2017
MoFe:Ni(OH) ₂ /NiOOH	240	295*	--	47	NF	17	2018
Cu@NiFe LDH	199	281	305*	27.8	Cu foam	1	2017

NiFe LDH@Au/Ni foam	--	235	250*	48.4	NF	18	2017
NiFeRu LDH/Ni foam	225	265*	280*	32.4	NF	19	2018
NiFe-Pt LDH	230	310*	--	33	CC ⁵	20	2017
ZnNi LDH/N-rGO	290	--	--	44	GC	21	2017
Exfoliated NiFe LDH	302	--	--	40	GC	22	2014
NiFe LDH/CNT	247	--	--	31	CFP	23	2013

Note: * The value is roughly calculated from the curves shown in the corresponding literature.

¹Nickel foam, ²Carbon fiber paper, ³Glassy carbon, ⁴Graphite foil, ⁵Carbon cloth.

Table S2. Comparison of HER performance for the Ni@NiFe LDH catalyst in this work with other recently reported electrocatalysts in 1 M KOH electrolyte.

Catalysts	η_{10} (mV)	Tafel Slope (mV·dec ⁻¹)	Substrate	Ref.	Year
Ni@NiFe LDH	92	72.3	NF¹	The Work	--
Ni _{0.75} Fe _{0.125} V _{0.125} -LDHs	125	62.0	NF	24	2017
Co _{0.85} Se/NiFe LDH/EG	260	160	GF ²	13	2016
Porous NiSe ₂ NSs	184	77	CFP ³	25	2015
Cu@NiFe LDH	116	58.9	Cu foam	1	2017
Ni ₅ P ₄ /NiP ₂ /NiFe LDH	124	--	NF	3	2018
NF@Ni/C	37	57.0	NF	4	2018
NiFe LDH@NiCoP/NF	120	88.2	NF	2	2018
NiCo ₂ P ₂ /GQD NSs	52	68.0	Ti mesh	5	2018
NiFe LDH NS@DG10	300	110	GC ⁴	12	2017
Ni _{0.9} Fe _{0.1} /NC	231	111	NF	26	2015
MoS ₂ /Ni ₃ S ₂ heterostructures	110	83.1	NF	27	2016

Note: ¹Nickel foam, ²Graphite foil, ³Carbon fiber paper, ⁴Glassy carbon.

Table S3. Comparison of OWS performance for the Ni@NiFe LDH catalyst in the work with other recently reported electrocatalysts in 1 M KOH electrolyte.

Catalysts	Voltage at 10 mA·cm ⁻² (V)	Substrate	Ref.	Year
Ni@NiFe LDH	1.53	NF¹	The Work	--

IrO₂ // Pt/C	1.55	NF	The Work	--
Ni _{0.75} Fe _{0.125} V _{0.125} -LDHs	1.59	NF	24	2017
Co _{0.85} Se/NiFe LDH/EG	1.67	GF ²	13	2016
Porous NiSe ₂ NSs	1.79*	CFP ³	25	2015
Cu@NiFe LDH	1.54	Cu foam	1	2017
Ni ₅ P ₄ /NiP ₂ /NiFe LDH	1.52	NF	3	2018
NiFe LDH@NiCoP/NF	1.57	NF	2	2018
NiCo ₂ P ₂ /GQD NSs	1.61	Ti mesh	5	2018
NiFe/NiCo ₂ O ₄ /Ni Foam	1.67	NF	28	2016
Ni _{0.9} Fe _{0.1} /NC	1.58	NF	26	2015
MoS ₂ /Ni ₃ S ₂ heterostructure	1.56	NF	27	2016

Note: * The value is roughly calculated from the curves shown in the corresponding literature.

¹Nickel foam, ²Graphite foil, ³Carbon fiber paper.

Reference

1. L. Yu, H. Zhou, J. Sun, F. Qin, F. Yu, J. Bao, Y. Yu, S. Chen and Z. Ren, *Energy Environ. Sci.*, 2017, **10**, 1820-1827.
2. H. Zhang, X. Li, A. Haehnel, V. Naumann, C. Lin, S. Azimi, S. L. Schweizer, A. W. Maijenburg and R. B. Wehrspohn, *Adv. Funct. Mater.*, 2018, **28**, 1706847.
3. L. Yu, H. Zhou, J. Sun, I. K. Mishra, D. Luo, F. Yu, Y. Yu, S. Chen and Z. Ren, *J. Mater. Chem. A*, 2018, **6**, 13619-13623.
4. H. Sun, Y. Lian, C. Yang, L. Xiong, P. Qi, Q. Mu, X. Zhao, J. Guo, Z. Deng and Y. Peng, *Energy Environ. Sci.*, 2018, **11**, 2363-2371.
5. J. Tian, J. Chen, J. Liu, Q. Tian and P. Chen, *Nano Energy*, 2018, **48**, 284-291.
6. L. Yu, H. Zhou, J. Sun, F. Qin, D. Luo, L. Xie, F. Yu, J. Bao, Y. Li, Y. Yu, S. Chen and Z. Ren, *Nano Energy*, 2017, **41**, 327-336.
7. C. Yu, Z. Liu, X. Han, H. Huang, C. Zhao, J. Yang and J. Qiu, *Carbon*, 2016, **110**, 1-7.
8. J. Li, W. Xu, R. Li, J. Luo, D. Zhou, S. Li, P. Cheng and D. Yuan, *J. Mater. Sci.*, 2016, **51**, 9287-9295.
9. J. Wu, Z. Ren, S. Du, L. Kong, B. Liu, W. Xi, J. Zhu and H. Fu, *Nano Research*, 2016, **9**, 713-725.
10. Y. Shao, M. Zheng, M. Cai, L. He and C. Xu, *Electrochim. Acta*, 2017, **257**, 1-8.
11. C. Zhang, M. Shao, L. Zhou, Z. Li, K. Xiao and M. Wei, *ACS Appl. Mater. Interfaces*, 2016, **8**, 33697-33703.
12. Y. Jia, L. Zhang, G. Gao, H. Chen, B. Wang, J. Zhou, M. T. Soo, M. Hong, X. Yan, G. Qian, J. Zou, A. Du and X. Yao, *Adv. Mater.*, 2017, **29**, 1700017.
13. Y. Hou, M. R. Lohe, J. Zhang, S. Liu, X. Zhuang and X. Feng, *Energy Environ. Sci.*, 2016, **9**, 478-483.
14. D. Zhao, K. Jiang, Y. Pi and X. Huang, *Chemcatchem*, 2017, **9**, 84-88.
15. Z. Lu, L. Qian, Y. Tian, Y. Li, X. Sun and X. Duan, *Chem. Commun.*, 2016, **52**, 908-911.
16. J. Yu, G. Cheng and W. Luo, *J. Mater. Chem. A*, 2017, **5**, 11229-11235.
17. Y. Jin, S. Huang, X. Yue, H. Du and P. K. Shen, *ACS Catal.*, 2018, **8**, 2359-2363.

18. W. Zhu, L. Liu, Z. Yue, W. Zhang, X. Yue, J. Wang, S. Yu, L. Wang and J. Wang, *ACS Appl. Mater. Interfaces*, 2017, **9**, 19807-19814.
19. G. Chen, T. Wang, J. Zhang, P. Liu, H. Sun, X. Zhuang, M. Chen and X. Feng, *Adv. Mater.*, 2018, **30**, 1706279.
20. S. Anantharaj, K. Karthick, M. Venkatesh, T. V. S. V. Simha, A. S. Salunke, L. Ma, H. Liang and S. Kundu, *Nano Energy*, 2017, **39**, 30-43.
21. A. Nadeema, V. M. Dhavale and S. Kurungot, *Nanoscale*, 2017, **9**, 12590-12600.
22. F. Song and X. Hu, *Nat. Commun.*, 2014, **5**, 4477.
23. M. Gong, Y. Li, H. Wang, Y. Liang, J. Z. Wu, J. Zhou, J. Wang, T. Regier, F. Wei and H. Dai, *J. Am. Chem. Soc.*, 2013, **135**, 8452-8455.
24. D. Khang Ngoc, P. Zheng, Z. Dai, Y. Zhang, R. Dangol, Y. Zheng, B. Li, Y. Zong and Q. Yan, *Small*, 2018, **14**, Unsp 1703257.
25. H. Liang, L. Li, F. Meng, L. Dang, J. Zhuo, A. Forticaux, Z. Wang and S. Jin, *Chem. Mater.*, 2015, **27**, 5702-5711.
26. X. Zhang, H. Xu, X. Li, Y. Li, T. Yang and Y. Liang, *ACS Catal.*, 2016, **6**, 580-588.
27. J. Zhang, T. Wang, D. Pohl, B. Rellinghaus, R. Dong, S. Liu, X. Zhuang and X. Feng, *Angew. Chem.*, 2016, **128**, 6814-6819.
28. C. Xiao, Y. Li, X. Lu and C. Zhao, *Adv. Funct. Mater.*, 2016, **26**, 3515-3523.